HHS Public Access

Author manuscript

Proc SPIE Int Soc Opt Eng. Author manuscript; available in PMC 2014 July 28.

Published in final edited form as:

Proc SPIE Int Soc Opt Eng. 2013 March 14; 8671: 86711Y–. doi:10.1117/12.2008157.

Quantitative evaluation of multi-parametric MR imaging marker changes post-laser interstitial ablation therapy (LITT) for epilepsy

Pallavi Tiwari[a], **Shabbar Danish**[b], **Stephen Wong**[b], and **Anant Madabhushi**[a]

[a]Department of Biomedical Engineering, Case Western Reserve University, Cleveland, OH USA

[b]Department of Neurology, University of Medicine and Dentistry, NJ, USA

Abstract

Laser-induced interstitial thermal therapy (LITT) has recently emerged as a new, less invasive alternative to craniotomy for treating epilepsy; which allows for focussed delivery of laser energy monitored in real time by MRI, for precise removal of the epileptogenic foci. Despite being minimally invasive, the effects of laser ablation on the epileptogenic foci (reflected by changes in MR imaging markers post-LITT) are currently unknown. In this work, we present a quantitative framework for evaluating LITT-related changes by quantifying per-voxel changes in MR imaging markers which may be more reflective of local treatment related changes (TRC) that occur post-LITT, as compared to the standard volumetric analysis which involves monitoring a more global volume change across pre-, and post-LITT MRI. Our framework focuses on three objectives: (a) development of temporal MRI signatures that characterize TRC corresponding to patients with seizure freedom by comparing differences in MR imaging markers and monitoring them over time, (b) identification of the optimal time point when early LITT induced effects (such as edema and mass effect) subside by monitoring TRC at subsequent time-points post-LITT, and (c) identification of contributions of individual MRI protocols towards characterizing LITT-TRC for epilepsy by identifying MR markers that change most dramatically over time and employ individual contributions to create a more optimal weighted MP-MRI temporal profile that can better characterize TRC compared to any individual imaging marker. A cohort of patients were monitored at different time points post-LITT via MP-MRI involving T1-w, T2-w, T2-GRE, T2-FLAIR, and apparent diffusion coefficient (ADC) protocols. Post affine registration of individual MRI protocols to a reference MRI protocol pre-LITT, differences in individual MR markers are computed on a per-voxel basis, at different time-points with respect to baseline (pre-LITT) MRI as well as across subsequent time-points. A time-dependent MRI profile corresponding to successful (seizure-free) is then created that captures changes in individual MR imaging markers over time. Our preliminary analysis on two patient studies suggests that (a) LITT related changes (attributed to swelling and edema) appear to subside within 4-weeks post-LITT, (b) ADC may be more sensitive for evaluating early TRC (upto 3-months), and T1-w may be more sensitive in evaluating early delayed TRC (1-month, 3-months), while T2-w and T2-FLAIR appeared to be more sensitive in identifying late TRC (around 6-months post-LITT) compared to the other MRI protocols under evaluation. T2-GRE was found to be only nominally sensitive in identifying TRC

Correspondence to [pallavi.tiwari@case.edu, anantm@case.edu].

at any follow-up time-point post-LITT. The framework presented in this work thus serves as an important precursor to a comprehensive treatment evaluation framework that can be used to identify sensitive MR markers corresponding to patient response (seizure-freedom or seizure recurrence), with an ultimate objective of making prognostic predictions about patient outcome post-LITT.

Keywords

laser interstitial thermal therapy; epilepsy; focal treatment; treatment change; registration; multi-parametric MRI; monitoring; treatment evaluation

1. INTRODUCTION

Epilepsy affects nearly 3 million people in the United States (U.S.) and 50 million people worldwide. [1] One-third of epilepsy patients have seizures that cannot be controlled by any antiepileptic drug treatment, [1] most of whom resort to open resection via craniotomy to potentially remove the primary epileptogenic focus. Engel [2] proposed a scheme which has become the de facto standard when evaluating postoperative outcomes for epilepsy surgery: free of disabling seizures (class I), rare disabling seizures ("almost seizure-free") (class II), worthwhile improvement (class III), and no worthwhile improvement (class IV). Class IV Engel outcome is shown to be significantly correlated with non-lesional resective procedures, and incompleteness of lesional resections [3] during craniotomy. A recent alternative to traditional craniotomy is minimally invasive laser-interstitial thermal therapy (LITT) which is a new exploratory method that attempts to ablate seizure foci with minimal damage to normal surrounding tissue. Since LITT is MRI compatible, accurate identification of the epileptogenic foci (which appears as atrophy on MRI) for precise thermal ablation of epileptogenic foci and avoiding critical structures is possible. [4] While LITT holds significant potential to be the treatment modality of choice for epilepsy, it is currently only practiced as an investigational procedure at a few centers worldwide. Consequently very little is known about its effects on the ablated epilepsy zone post-treatment. [5]

MRI, due to its high resolution and ability to acquire simultaneous multi-parametric (MP) structural and functional information, has been the standard of care for diagnostic and treatment evaluation purposes for neuroimaging applications for over a decade. [6-9] In the context of LITT, epilepsy patients are monitored qualitatively via volumetric analysis on T1-w MRI protocol. [4] T1-w MRI allows for capture of volume of enhancement within epileptogenic focus post-treatment, acquired at regular time intervals (24-hours, 1-month, 3-months, 6-months post-treatment) and comparing these changes with reference to pre-treatment T1-w MRI to identify patients who may still be prone to seizure persistence. [4] The volumetric analysis (known as MacDonald criterion [7]) however may be sub-optimal in precisely localizing specific LITT related changes on MRI since it involves evaluating a single parameter (volume) to detect changes pre-, and post-MRI. The availability of MP-MRI protocols acquired at multiple time points post-LITT (24-hours, 1-month, 3-months, 6-months, and so on) provides us with a unique opportunity to evaluate and monitor per-voxel changes across MRI protocols over time, and identify MRI markers that correspond to

treatment related changes (TRC) (such as swelling, edema, seizure recurrence, and irreversible tissue damage) which present themselves as early-, mid-, and delayed-effects. [10,11] The changes in MR imaging markers corresponding to these TRC can serve as a surrogate of treatment response for identification of patients with successful treatment (class I Engel outcome) as against patients with seizure recurrence (II, III, or IV Engel outcome). The regular monitoring of MP-MRI markers may also provide us with additional insights on subtle changes in imaging markers that occur within the first few weeks due to the immediate effects of treatment. A temporal analysis of changes in MR markers can allow for identification of an optimal time-point when these early effects of treatment (such as edema and mass effect) subside and in turn assist in early identification of patients with seizure recurrence who may need additional intervention and/or supplemental drug therapy. There is hence a significant need for a framework that allows for evaluation and monitoring of voxel-level changes in imaging markers over time across MP-MRI, and identify sensitive MRI markers that correspond to early-, mid-, and delayed TRC post-LITT. [12]

Automated quantitative assessment of changes in MP-MRI imaging markers may provide the necessary framework for such an analysis for (a) early, accurate, and precise identification of MR imaging markers, on a per-voxel basis, that correspond to TRC in patients with successful (seizure free, Engel I outcome) or failed LITT treatment (Engel II, III, IV outcome), (b) identification of MRI markers that may be better suited for detection of different types of TRC (such as seizure recurrence, and irreversible tissue damage), [13] (c) identification of optimal time-point when early TRC subside, and (d) development of temporal MP-MRI profiles corresponding to a patient's response to therapy that can be used to train a prognostic classifier for early identification of patients with unsuccessful treatment (seizure persistence) against patients with seizure-free survival. The quantitative evaluation of TRC on MRI can be achieved by comparing changes in MR imaging markers, on a per-voxel basis, over time with respect to pre-LITT (baseline) MRI and across subsequent time-points to understand and monitor how and when the TRC post-LITT occur. However, there are a few challenges associated with developing such a quantitative framework including, (a) accurate alignment of various MR imaging protocols at different time-points via registration for computing voxel level differences of the imaging markers (reflective of TRC), (b) identification of the "most sensitive" imaging marker changes corresponding to TRC across different MR protocols at different time-points, and (c) integrating changes in imaging markers and thereby identify imaging biomarkers reflective of successful or failed treatment.

In this work we present a first-of-its-kind quantitative framework for evaluating LITT related changes, that has embedded within it, (a) co-registration tools to accurately align MP-MRI protocols pre- and post-LITT, to allow for accurate per-voxel quantification of differences in corresponding image intensities on individual MP-MRI protocols (T1-w, T2-w, T2-GRE, T2-FLAIR, and ADC) over time, (b) creating MR imaging marker difference maps by computing differences in structural and functional markers across MP-MRI protocols, with respect to baseline (pre-LITT) MR as well as across subsequent time-points, (c) identifying sensitive MR imaging markers that change most-dramatically over time while computing TRC post-LITT, (d) identifying an optimal time point when early treatment induced changes subside, and (e) developing a weighted temporal MP-MRI signature

corresponding to seizure freedom (favorable outcome), by optimally combining the imaging markers identified as most sensitive in evaluating TRC at different time-points post-LITT. The framework presented in this work could be extended for evaluation of imaging marker changes within a larger cohort of studies to develop temporal signatures corresponding to Engel I, II, III, and IV outcomes, which could then be used to train a prognostic classifier to predict a patient's LITT outcome.

The remainder of the paper is organized as follows. Section 2 discusses the rationale and objectives of this work. In Section 3, we provide methodological details associated with each of the objectives of this work. Experimental results are presented in Section 4. We provide concluding remarks in Section 5.

2. RATIONALE AND OBJECTIVES OF THIS WORK

In the context of cancer types such as brain tumor [6,8,9,14] and prostate cancer, [12,15] a recent focus has been on quantitative monitoring of changes in MP-MRI markers post-radiation therapy (RT) with respect to baseline (pre-treatment) MRI. The objective of such quantitative monitoring of MRI markers is to identify sensitive MR markers corresponding to specific TRC over time which can serve as prognostic markers of a patient's response to the treatment.

Identifying changes in MR imaging markers for studying a patient's response to treatment

A recent work by Jamin et al [9] involved studying significant changes in native relaxation times T1 and T2, the relaxation rate R2*, and dynamic contrast-enhanced MRI between pre-, and post-treatment imaging to monitor tumor response to different drugs in a transgenic mouse model of neuroblastoma. T1 relaxation time was identified as a robust noninvasive imaging biomarker for studying drug response in TH-MYCN mice (known to emulate high-risk neuroblastoma in children). Another recent study involving head and neck cancers [16] evaluated changes in T2-w MR intensities to study early post-chemo-RT (CRT) assessment of the primary tumor. The study demonstrated the efficacy of T2-w MRI in accurately localizing early CRT changes within 8-weeks post-CRT. Chan et al. [17] studied morphological characteristics of late radiation induced changes on T1-w spin echo, T2-w spin-echo, GRE, FLAIR and T1-w post-contrast sequences demonstrating that the late effects of radiation are more varied on MP-MRI than have been reported in the literature.

Identifying changes in MR imaging markers for predicting a patient's outcome

Khayal et al. [6] investigated changes in diffusion parameters at pre-, mid-, and post-RT for post-surgical Glioblastoma (GBM) patients to identify imaging markers that correspond to long-term patient survival. The results suggested that the changes in mid- to post-RT were significantly different between patients who progressed within 6-months versus those who were free of progression for 6-months after initiation of therapy. A detailed overview of the use of diffusion MRI as a surrogate marker for quantifying treatment responsiveness in both preclinical and clinical studies is provided in Ross et al. [8] In Pope et al., [14] ADC histogram analysis was used to compare post- and pre-treatment ADC values to stratify patients with 6 month progression-free survival against patients with recurrent GBM.

Identifying the appropriate time-point when early changes induced due to therapy dissipate

Foltz et al. [15] evaluated short-term TRC by evaluating changes in values of ADC and T2 relaxation every 2 weeks with respect to baseline-MRI, over the course of 8 weeks. The significant findings of the work by Foltz et al. included, (a) identifying MRI marker changes that were found to be correlated to specific TRC, and (b) identifying an optimal time-point since initiation of treatment, when treatment failed (known as biochemical failure). Performing such an extensive quantitative evaluation across MP-MRI at different time-points could be significant in that it provides clinicians with clinical insights on, (a) changes in imaging markers as a function of time and how they relate to a patient's response to treatment, (b) identification of the MR protocol that is potentially more informative in identifying a specific TRC, and (c) allows for a more careful monitoring of changes in imaging markers at the optimal time point at which early TRC subside and changes due to failed treatment may become discernible.

2.1 Objectives of this work

To our knowledge the work presented here represents the first attempt at evaluating the efficacy of the new promising treatment modality, LITT, and understanding and evaluating its effects on epilepsy patients post-LITT. Based on the findings of Khayal et al. [6] and Foltz et al., [15] in this work, we address the following questions pertinent in the context of evaluating TRC post-LITT: (1) Can we identify specific imaging signatures that reflect changes in MRI markers over time for identification of patients with Engel I outcome against patients with Engel II, III or IV outcome?, (2) Can we identify an optimal time point when early LITT-induced thermal effects subside to allow for identification of early signs of failed treatment? and (3) Can we identify individual contributions of MRI markers in accurately quantifying TRC over time? In this work, we develop a novel quantitative framework which focuses on studying the following three objectives in the context of studying precise LITT-induced changes post-LITT,

1. To compute a temporal MRI profile that characterizes TRC corresponding to patients with seizure freedom by computing differences of MR imaging marker changes and monitoring them over time,
2. To identify the optimal time point when early LITT induced effects subside by monitoring TRC at subsequent time-points post-LITT, and
3. To identify contributions of individual MRI protocols towards characterizing LITT-TRC for epilepsy by identifying MR markers that change most dramatically over time, and employ individual contributions to create a more optimal weighted MP-MRI temporal profile that can better characterize TRC compared to any individual imaging marker.

3. METHODOLOGY

3.1 Dataset Description

An FDA-cleared surgical laser ablation system (Visualase Thermal Therapy System; Visualase, Inc., Houston, TX) was employed for the LITT procedure. Two epilepsy patients were monitored post-LITT via MP-MRI (T1-w, T2-w, GRE, FLAIR, and ADC) as a part of an ongoing study at University of Medicine and Dentistry, New Jersey (UMDNJ) between 2011-2012, after initial 3-Tesla MP-MRI. Post-LITT, patient 1 (D_1) was reimaged after 24-hours, 1-month, 3-months, and 6-months while patient 2 (D_2) was reimaged after 24-hours, 2-months, and 6-months with both identified as favorable outcome (seizure freedom (S.F.)). Details on available protocols and time-points for D_1, and D_2 is provided in Table 1.

3.2 Notation

We denote $\mathscr{C}_{T1}^{t_0}$ as a 3D grid for T1-w MRI protocol pre-LITT. The remaining pre-LITT protocols are registered to $\mathscr{C}_{T1}^{t_0}$ to obtain, $\mathscr{C}_i^{t_0} = \left(C_i, f_i^{t_0}\right)$ where $f_i^{t_0}(c)$ is the associated intensity at every voxel location c on a 3D grid C_i, $i \in \{T2, GRE, FLAIR, ADC\}$. The ablation zone on every 3D MRI grid is defined as G, where $\mathscr{G} \subset \mathscr{C}$. A detailed list of all the notations used in this paper are provided in Table 2.

Figure 1 presents an overview of our framework illustrating modules for each of the three objectives. Each objective and associated methodology is described in more details in the following subsections.

3.3 Objective 1: To create a temporal profile of MR imaging marker changes correlated to post-LITT seizure freedom

3.3.1 Module 1: Co-Registration of multi-parametric MRI between baseline-MRI ($\mathscr{C}^{t_0}$) and across different time-points ($\mathscr{C}^{t_k}$))—After pre-processing each of the MRI protocols for bias-field correction and intensity standardization, a 3D affine transformation with 12 degrees of freedom, encoding rotation, translation, shear, and scale, was employed to accurately align post-LITT brain MRI with reference to $\mathscr{C}_{T1}^{t_0}$, which yielded a registered 3D volume, $\mathscr{C}_i^{t_k}$, at every time-point t_k, $k \in \{1, \ldots, n\}$, n being the total number of time points evaluated post-LITT, for every i, $i \in \{T1, T2, GRE, FLAIR, ADC\}$. During registration, the 3D volume is appropriately resampled and interpolated, in order to account for varying voxel sizes and resolutions between different time-points and protocols. Note that all the different MP-MRI acquisitions are aligned to the pre-treatment frame of reference $\mathscr{C}_{T1}^{t_0}$ to enable per-voxel quantitative comparisons across different time-points and protocols post-LITT (Figure 1(a)).

3.3.2 Module 2: Generating difference maps for each time point with respect to baseline-MRI for individual protocols—Post-registration, a differences map is computed for every $c \in \mathscr{G}$, $c \in \mathscr{G}$ as, $\mathscr{G} \subset \mathscr{C}$, where $\Delta_i^k = \| \mathscr{G}_i^{t_0} - \mathscr{G}_i^{t_k} \|_1$ is the time point post-LITT, $i \in \{T1, T2, GRE, FLAIR, ADC\}$ is the imaging protocol evaluated is the post-LITT, $\mathscr{C}_i^{t_0}$ is the baseline-MRI for protocol i, and $\|.\|_1$ represents the L_1 norm. Individual

difference maps (Δ_i, $i \in \{T1, T2, GRE, FLAIR, ADC\}$) allow for quantification of changes in imaging markers with respect to baseline (pre-LITT) MRI across each of the individual protocols.

3.3.3 Module 3: Generating a temporal profile for capturing MP-MRI differences across time-points with baseline-MRI—For a specific protocol, i, $i \in \{T1, T2, ADC, GRE, FLAIR\}$ and for every $c \in \mathcal{G}$, where $\mathcal{G} \subset \mathcal{C}$, the average intensity $\mu_i(t_k) = \frac{1}{N}\sum_N \left(\Delta_i^k\right)$ is computed, such that $N = |\mathcal{G}|$ is the cardinality of G. We then develop a temporal MRI profile for every at every i as $\delta_i = [\mu_i(t_1), \mu_i(t_2), \ldots \mu_i(t_n)]$ by plotting μ_i at every time-point t_k, $k \in \{1,2, \ldots, n\}$.

3.4 Objective 2: Identify an optimal time-point at which early LITT TRC subside on MRI

Module 1: Co-Registration of MP-MRI protocols across subsequent time-points: $\mathcal{C}_i^{t_k}$ at every time-point t_k, $k \in \{1,2, \ldots, n\}$, is registered with reference to $\mathcal{C}_i^{t_0}$, n is the total number of time points evaluated post-LITT, for every i, $i \in \{T1, T2, GRE, FLAIR, ADC\}$ using the methods illustrated in Section 3.3.1. The registration with reference to $\mathcal{C}_{T1}^{t_0}$ allows for alignment of all protocols across different time-points in the same frame of reference for a voxel-by-voxel comparison.

3.4.1 Module 2: Generating difference maps for individual protocols—A differences map is computed for every $c \in \mathcal{G}, \mathcal{G} \subset \mathcal{C}$ as, $\tilde{\Delta}_i^k = |\mathcal{G}_i^{t_k} - \mathcal{G}_i^{t_{k+1}}|$, where $k \in \{1, \ldots, n\}$, is the time point post-LITT, $i \in \{T1, T2, GRE, FLAIR, ADC\}$ is the imaging protocol evaluated, and $\|.\|$ represents the L_1, norm. Individual MRI parameter difference maps ($\tilde{\Delta}_i$, $i \in \{T1, T2, GRE, FLAIR, ADC\}$) allow for quantification of changes in imaging markers across subsequent time-points.

3.4.2 Module 3: Evaluating temporal profiles of MRI markers—For a specific protocol, i, $i \in \{T1, T2, ADC, GRE, FLAIR\}$, and for every $c \in \mathcal{G}$, where $\mathcal{G} \subset \mathcal{C}$, the average intensity $\tilde{\mu}_i(t_k) = \frac{1}{N}\sum_N \left(\tilde{\Delta}_i^k\right)$ is computed, such that $N = |\mathcal{G}|$, and $|.|$ is the cardinality of G. We then develop a temporal MRI profile for every i as $\tilde{\delta}_i = [\tilde{\mu}_i(t_1), \tilde{\mu}_i(t_2), \ldots, \tilde{\mu}_i(t_n)]$, by plotting $\tilde{\mu}_i$ at every time-point, t_k, $k \in \{1,2, \ldots, n\}$.

3.5 Objective 3: Evaluating extent of changes in individual MRI markers post-LITT for epilepsy

3.5.1 Module 1: Co-Registration of multi-parametric MRI across time points—For a specific time-point, t_k, $k \in \{1,2, \ldots, n\}$, each of $\mathcal{C}_i^{t_k}$, $i \in \{T1, T2, ADC, GRE, FLAIR\}$ is individually registered to $\mathcal{C}_{T1}^{t_0}$ as described in Section 3.3.1 to align all MRI protocols across multiple time-points to a common frame of reference.

3.5.2 Module 2: Generating a multi-parametric weighted MRI map—The relative contribution of each protocol is obtained by identifying MR markers that change most

dramatically post-LITT and hence may serve as more sensitive markers in capturing TRC. We hypothesize that greater the change in an imaging marker as a function of TRC, the higher the likelihood that it is a sensitive marker reflective of TRC. The individual contributions are obtained for each protocol depending on their sensitivity in capturing TRC and are combined to develop an integrated MP-MRI meta-marker that simultaneously captures the discriminability in changes across all individual MRI markers. We believe that such a meta-marker will be more sensitive and specific to true treatment related changes compared to looking at changes across individual markers.

A weighted MP-MRI meta-marker map is obtained by leveraging difference maps for each of the protocols as, $\mathscr{C}^k_{map}=\sum_{v=1}^{J}\alpha_v^k\Delta_v^k$, where α_v^k weights the relative contribution of each of the individual imaging markers at every time point, k, $k \in \{1,2, \ldots, n\}$, and J is the total number of imaging markers under evaluation.

The optimal weights for each of the individual MRI protocols were obtained via a grid search strategy. [18] The weights for each of the 5 protocols were varied between 0 and 1 in the increments of 0.2, such that $\sum_{i=1}^{J}\alpha_i=1$, which resulted in a total of 125 weighted combinations of MP-MRI profiles (J = 5). The top 20% of the 125 MP-MRI profiles that changed most drastically over time were selected (yielding 25 candidate profiles) such that changes in Δ^1_{map} are elevated, and reduced in Δ^2_{map}, Δ^3_{map}, and Δ^4_{map}. A voting scheme was then implemented to determine the protocols that occurred most frequently across the 25 candidate profiles, and the weight for each protocol (normalized between 0 and 1) was assigned based on its frequency of occurrence across the 25 profiles, at each time-point.

3.5.3 Module 3: Generating a temporal weighted MP-MRI profile that captures combined differences of imaging markers with respect to baseline-MRI—For a specific protocol, i, $i \in \{T1, T2, ADC, GRE, FLAIR\}$, and for every $c \in \mathscr{G}$, where $\mathscr{G} \in \mathscr{C}$, the average intensity $\mu_{map}(t_k)=\frac{1}{N}\sum_N\left(\Delta^k_{map}\right)$ is computed such that $N=|\Delta^k_{map}|$, and $|.|$ is the cardinality of G. We then develop an integrated temporal profile as δ_{map} = [$\mu_{map}(t_1)$, $\mu_{map}(t_2)$, … $\mu_{map}(t_n)$], by plotting μ_{map} at every time-point t_k, $k \in \{1,2, \ldots, n\}$.

4. EXPERIMENTAL RESULTS

4.1 Implementation details

The initial pre-processing (intensity normalization and bias field correction) along with the co-registration across different MRI sequences were implemented via the 3D Slicer software 4.1. (http://www.slicer.org/). Modules 2 and 3 of each of the three objectives involving computation of difference maps, development of temporal signatures, optimization and integration of weights across different MRI protocols were implemented via the Matlab software package.

4.2 Objective 1: To create a temporal profile of MR imaging marker changes correlated to post-LITT seizure freedom

Figure 2 shows changes across one-protocol (T2-w MRI intensities) at different time-points with respect to baseline-MRI. The original T2-w MRI images for baseline (pre-LITT), 24-hour, 1-month, 3-months, and 6 months are shown in Figures 2 (a), (b), (c), (d), and (e) respectively, while the difference maps with respect to baseline for each of 24-hour (Δ^1_{T2}), 1-month (Δ^2_{T2}), 3-months (Δ^3_{T2}), and 6-months (Δ^4_{T2}) are shown in Figures 2 (f), (g), and (h) respectively. Mean intensity μ_i^k, for each Δ_i^k is obtained within the epileptogenic focus for every *i*,$i \in \{T2,T2,FLAIR,GRE,ADC\}$, and recorded over different time-points, $k \in \{1,2,3,4\}$. Figure 2 (j) shows different temporal profiles (normalized between 0 and 1) created for each of the protocols for D_1 obtained by plotting μ_i^k at every time-point *k*. Similar trends in temporal profiles for MR protocols were obtained for D_2. Figure 2 further suggests that, (a) intensity differences consistently decrease over all protocols for patients with successful treatment, and (b) the intensity differences after 1-month are considerably reduced as compared to that within the first 1-month.

4.3 Objective 2: Identify an optimal time-point at which early LITT TRC subside on MRI

Figure 3 shows difference maps obtained across multiple time-points for the T2-w MRI protocol. Figures 3(a)-(d) show the original T2-w MRI slices containing the ablation zone for 24-hours, 1-month, 3-months, and 6-months respectively, while the corresponding difference maps, $\tilde{\Delta}_1$, $\tilde{\Delta}_2$ and $\tilde{\Delta}_3$ are shown in Figures 3(e), (f), and (g) respectively. Temporal signatures, $\tilde{\delta}_i$ for every *i*,$i \in \{T1,T2,ADC,GRE,FLAIR\}$, are shown in different colors in Figure 3(h), obtained by plotting $\tilde{\mu}_i^k$ at every time-point t_k, $k \in \{1,2,3,4\}$ Note how the changes are more prominent between $\tilde{\Delta}_1$ as compared to $\tilde{\Delta}_2$, and $\tilde{\Delta}_3$. This appears to suggest that most of the early LITT effects occur and subside within the first one month, and the structural intensities appear to return to pre-LITT MR intensities following the 4 weeks post-LITT. Based on clinical findings, [4] the exaggerated changes in MP-MRI markers during the first one month may be attributed to edema and swelling caused due to the LITT treatment.

4.4 Objective 3: Evaluating extent of changes in individual MRI markers post-LITT for epilepsy

4.4.1 Identifying contributions of individual protocols in characterizing TRC post-LITT—Figure 4 illustrates the contributions of each of the protocols, based on the voting scheme, described in Section 3.5.2. The weights of the individual MRI markers were normalized between 0 and 1 over the two studies for different time points. The top 25 profiles with highest mean intensity differences for $\Delta^{t_1}_{MP}$ and lowest mean intensity differences for Δ^{t2}_{MP},Δ^{t3}_{MP}, Δ^4_{MP} were identified (based on the trends observed in Figure 2(j)), and the protocols that most commonly occurred over the top 25 weight profiles were identified as most “sensitive”.

Figure 4 illustrates that, ADC was identified as being most sensitive in capturing early TRC (upto 3-months), while T1 was found to be more sensitive in evaluating early delayed TRC (1-month, 3-months) compared to the other protocols under evaluation. T2 and FLAIR appear to be more sensitive of identifying late TRC (around 6-months post-LITT) as compared to ADC, GRE, and FLAIR, while GRE is only nominally sensitive in identifying TRC at any follow-up time-point post-LITT. These findings although limited to two studies appear to provide some preliminary insights on the sensitivity of the different MR protocols in evaluating TRC at different time-points.

4.4.2 Creating a weighted MP-MRI profile via integrating the weighted contributions of individual MRI markers—

Figure 5 shows difference maps Δ^1_{T1}, and Δ^1_{T2} and Δ^1_{ADC} for each of the different MRI protocols obtained by computing differences in image intensities at 24-hours with respect to the baseline scan. Similar difference maps for each of the protocols for image intensity differences at 1-month with respect to baseline, at 3-months with respect to baseline, and at 6-months with respect to baseline are shown in Figures 5 (g)-(k), (m)-(q), and (s)-(w) respectively. Figures 5 (f), (l), (r), and (x) show the corresponding weighted MP-MRI difference maps obtained as a weighted combination of imaging markers as illustrated in Figure 4. Note how imaging protocols change over time and contribute (depending on their sensitivity in capturing TRC) towards creating a MP-MRI meta-marker which appears to be more sensitive and specific to capturing specific TRC compared to changes across individual markers. Corresponding temporal MP-MRI profile obtained by the optimal weights is shown in Figure 2(j) as a dotted black line.

5. CONCLUDING REMARKS

LITT holds tremendous potential as a minimally invasive treatment modality for epilepsy. However, a more widespread adoption of this new, exciting technique would involve rigorous quantitative evaluation of its treatment related effects, which may be reflected via the changes in MR imaging markers post-LITT. Towards this end, we presented a novel framework for quantitatively evaluating MP-MR imaging marker changes post-LITT on a voxel-by-voxel basis, to identify the MR imaging markers that change most-dramatically post-LITT and hence may be more sensitive towards capturing TRC post-LITT. Our framework focused on three objectives, (a) to develop temporal MRI signatures that characterize TRC corresponding to patients with seizure freedom by comparing differences in MR imaging markers and monitoring them over time, (b) to identify the optimal time point when early LITT induced effects (such as edema and mass effect) subside by monitoring TRC at subsequent time-points post-LITT, and (c) to identify contributions of individual MRI protocols towards characterizing LITT-TRC for epilepsy by identifying MR markers that change most dramatically over time and employ individual contributions to create a more optimal weighted MP-MRI temporal profile that can better characterize TRC compared to any individual imaging marker.

Towards each of these objectives, we developed a temporal weighted MP-MRI profile that reflects changes in MP-MRI over time corresponding to seizure-free survival. This temporal analysis could be extended to learn temporal profiles in patients who are not responsive to

LITT, and further to train a prognostic classifier to make early predictions regarding a patient's outcome post-LITT. Our preliminary analysis on two patient studies suggested that LITT related changes appeared to subside in a period of 4 weeks following LITT. Additionally, we found that ADC may be more sensitive towards capturing early TRC (upto 3-months), while T1 may be more sensitive towards capturing early delayed TRC (1-month, 3-months), compared to the other MRI protocols under evaluation. Similarly, T2 and FLAIR appeared to be more sensitive in identifying late TRC (around 6-months post-LITT), while GRE was found to be only nominally sensitive in identifying TRC at any follow-up time-point post-LITT.

Although the preliminary analysis on evaluating TRC post-LITT on MP-MRI across different time-points have yielded encouraging results on two patient studies, we also acknowledge a few limitations of our study. Only two patient studies with favorable outcome were available for analysis. In the absence of patient data for unfavorable patient response (seizure recurrence), the temporal profile for favorable outcome developed in this work could not be validated, and hence its efficacy in capturing TRC corresponding to seizure freedom remains to be verified in a future study. Intensity standardization specific to different zones in the brain (such as grey and white matter) was not performed in this work. In future we intend to align and compare intensity profiles corresponding to each of the different zones in the brain across different time-points for improved intensity standardization. We also intend to examine temporal MP-MRI profiles corresponding to epilepsy persistence, and irreversible thermal damage to predict patient outcome. We will also extend this framework towards identifying temporal signatures to (1) model tumor growth on MP-MRI towards early prediction of the disease, and (2) studying treatment response in patients with primary and metastatic brain tumor for early detection of tumor recurrence.

ACKNOWLEDGMENTS

This work was made possible by grants from the National Institute of Health (R01CA136535, R01CA140772, R43EB015199, R21CA167811), National Science Foundation (IIP-1248316), and the QED award from the University City Science Center and Rutgers University.

REFERENCES

[1]. Tllez-Zenteno J, Hernndez Ronquillo L, Moien-Afshari F, Wiebe S. Surgical outcomes in lesional and non-lesional epilepsy: A systematic review and meta-analysis. Epilepsy Research. 2010; 89(23):310–318. [PubMed: 20227852]

[2]. Tonini C, Beghi E, Berg A, Bogliun G, Giordano L, Newton R, Tetto A, Vitezic D, Wiebe S. Predictors of epilepsy surgery outcome: a meta-analysis. Epilepsy research. 2004; 62(1):7587. E, V.

[3]. Engel, J. surgical treatment of the epilepsies [book]. Lippincott Williams and Wilkins; 1993.

[4]. Curry D, Gowda A, McNichols R, Wilfong A. MR-guided laser ablation of epileptogenic foci in children. Epilepsy and Behavior. 2012; 24:408–414. [PubMed: 22687387]

[5]. Schulze P, Adams V, Busert C, Bettag M, Kahn T, Schober R. Effects of Laser-induced Thermotherapy (LITT) on proliferation and apoptosis of glioma cells in rat brain transplantation tumors. Lasers Surg Med. 2002; 30:227–232. [PubMed: 11891743]

[6]. Khayal I, Polley M, Jalbert L, Elkhaled A, Chang S, Cha S, Butowski N, Nelson S. Evaluation of diffusion parameters as early biomarkers of disease progression in glioblastoma multiforme. Neuro Oncology. 2010; 12(9):908–916. [PubMed: 20501631]

[7]. Macdonald D, Cascino T, Schold S, Cairncross J. Response criteria for phase ii studies of malignant glioma. J Clin Oncol. 1990; 8:127780.

[8]. Ross B, Moffat B, Lawrence T, Mukherji S, Gebarski S, Quint D, Johnson T, Junck L, Robertson P, Muraszko K, Dong Q, Meyer C, Bland P, McConville P, Geng H, Rehemtulla A, Chenevert T. Evaluation of cancer therapy using di usion magnetic resonance imaging. Mol Cancer Ther. 2003; 2(6):581–587. [PubMed: 12813138]

[9]. Jamin Y, Tucker E, Poon E, Popov S, Vaughan L, Boult J, Webber H, Hallsworth A, Baker L, Koh D, Pearson A, Chesler L, Robinson S. Evaluation of clinically translatable MR imaging biomarkers of therapeutic response in the th-mycn transgenic mouse model of neuroblastoma. Radiology. 2013; 266:130–140. C, J. [PubMed: 23169794]

[10]. Morrison P, Jolesz F, Charous D, Mulkern R, an Hushek S, Margolis R, Fried M. MRI of Laser-induced Interstitial Thermal Injury in an in-vivo animal liver model with histologic correlation. J Magn Reson Imaging. 1998; 8:57–63. [PubMed: 9500261]

[11]. Mller-Lisse G, Heuck A, Stehling M, Frimberger M, Thoma M, Schneede P, Muschter R, Hofstetter A, Reiser M. Mri monitoring before, during and after interstitial laser-induced hyperthermia of benign prostatic hyperplasia. initial clinical experiences. Radiology. 1996; 36(9): 722–731.

[12]. Tiwari P, Viswanath S, Kurhanewicz J, Madabhushi A. Weighted combination of multi-parametric mr imaging markers for evaluating radiation therapy related changes in the prostate. Prostate Cancer Imaging. Image Analysis and Image-Guided Interventions, Proc. in MICCAI. 2011; 6963:80–91.

[13]. Tiwari P, Viswanath S, Kurhanewicz J, Sridhar A, Madabhushi A. Multimodal wavelet embedding representation for data combination (maweric): integrating MRI and spectroscopy for prostate cancer detection. NMR in Biomedicine. 2012; 25(4):607–619. [PubMed: 21960175]

[14]. Pope W, Kim H, Huo J, Alger J, Brown M, Gjertson D, Sai V, Young J, Tekchandani L, Cloughesy T, Mischel P, Lai A, Nghiemphu P, Rahmanuddin S. Recurrent glioblastoma multiforme: ADC histogram analysis predicts response to bevacizumab treatment. Radiology. 2009; 252(1):182–189. J, G. [PubMed: 19561256]

[15]. Foltz W, Wu A, Chung P, Catton C, Bayley A, Milosevic M, Bristow R, Warde P, Simeonov A, Jaffray D, Haider M, Mnard C. Changes in apparent di usion coefficient and t2 relaxation during radiotherapy for prostate cancer. Journal of Magnetic Resonance Imaging. 2012 Epub ahead of print.

[16]. King A, Keung C, Yu K, Mo F, Bhatia K, Yeung D, Tse G, Vlantis A, Ahuja A. T2-weighted MR imaging early after chemoradiotherapy to evaluate treatment response in head and neck squamous cell carcinoma. American Society of Neuroradiology. 2013 Epub ahead of print.

[17]. Chan Y, Leung S, King A, Choi P, Metreweli C. Late radiation injury to the temporal lobes: Morphologic evaluation at MR imaging. Radiology. 1999; 213(3):800–807. [PubMed: 10580956]

[18]. Bishop, C. pattern recognition and machine learning [book]. 2006.

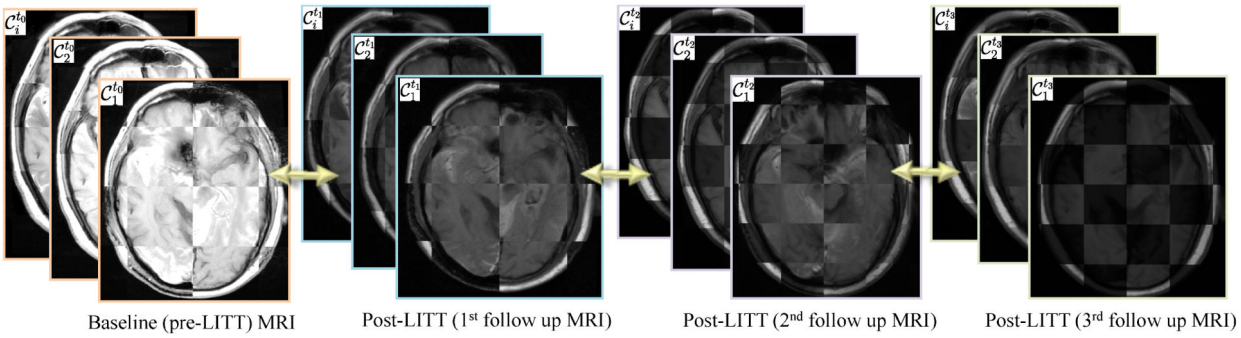

(a) Module 1: Registration

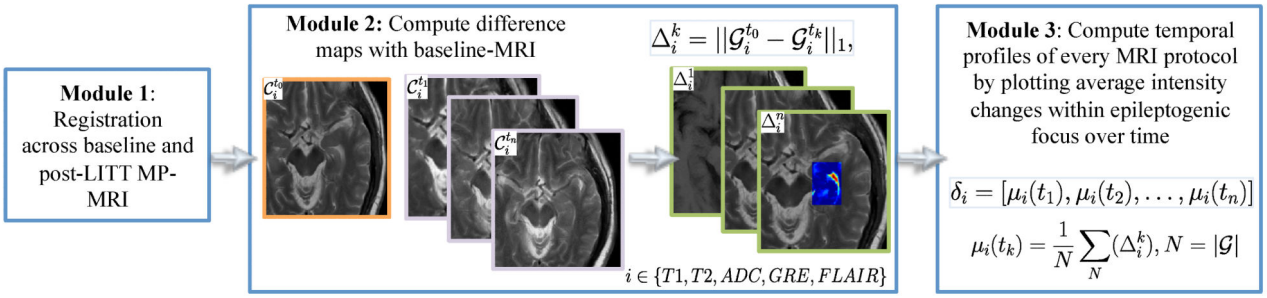

(b)

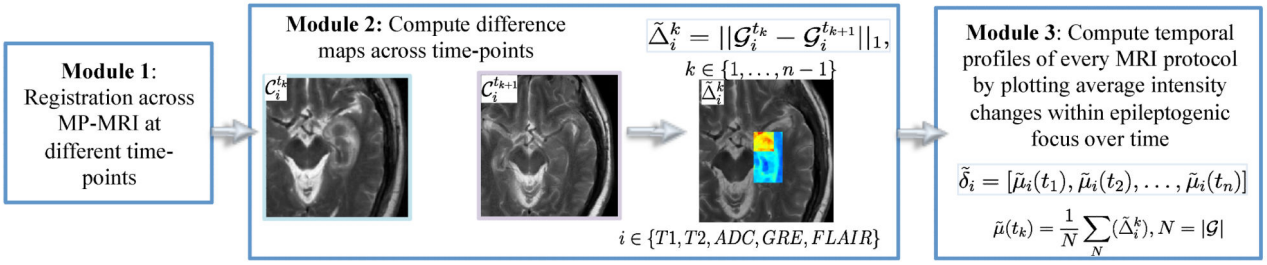

(c)

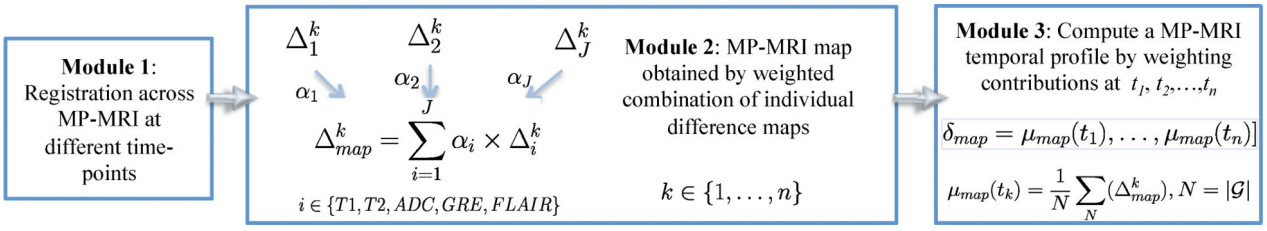

(d)

Figure 1.

Flowchart showing different modules for each of the three objectives, where (a) shows the registration module (module 1) which is integral to all the three objectives, (b) illustrates the methods for objective 1 to obtain a temporal MP-MRI signature of differences plotted with respect to baseline, while (c) illustrates the methods for objective 2 involving obtaining a temporal MRI signature of differences plotted at subsequent time-points. Figure 1(d) illustrates the methods for objective 3 involving developing an integrated MP-MRI signature by computing a weighted combination of MRI protocols at different time-points.

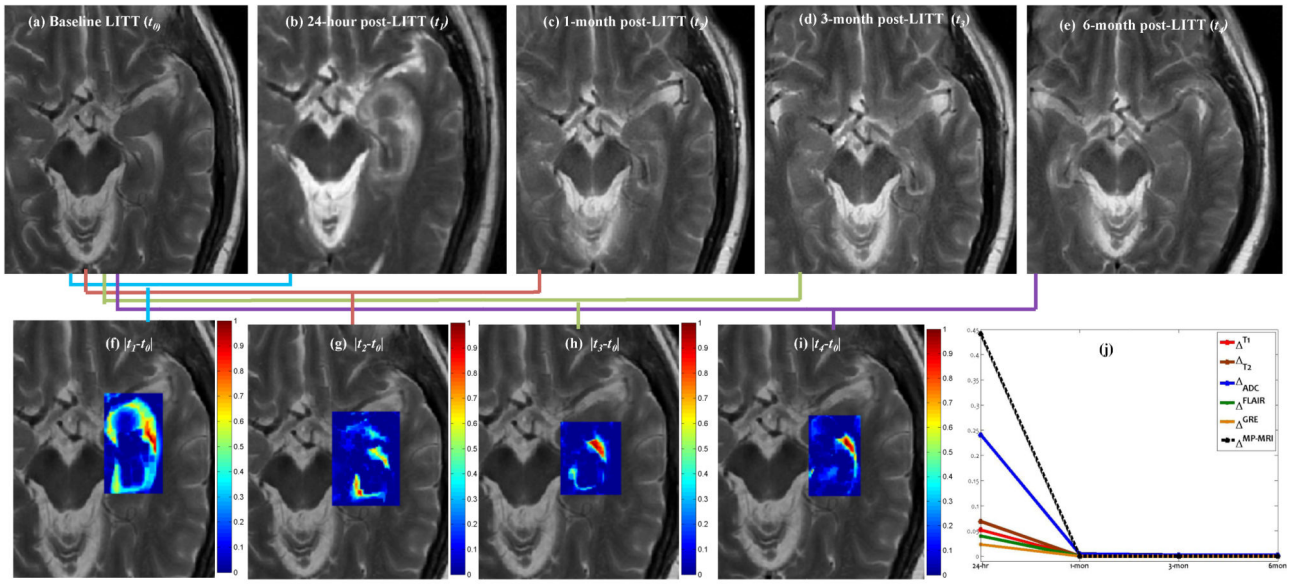

Figure 2.

Original T2-w MRI images for (a) baseline (pre-LITT), (b) 24-hour, (c) 1-month, (d) 3-month, (e) 6 month post-LITT. Figures 2(f)Δ_2, (g)Δ_3, (h) Δ_3, and (i) Δ_4 correspond to difference maps for T2-w MRI acquired at each of t_1, t_2, t_3 and t_4 with respect to t_0. Figure 2(j) shows temporal profiles of every MR protocol $i,i \in \{T1,T2,ADC,GRE,FLAIR\}$ reflecting the changes in imaging markers at different time-points with respect to baseline scan.

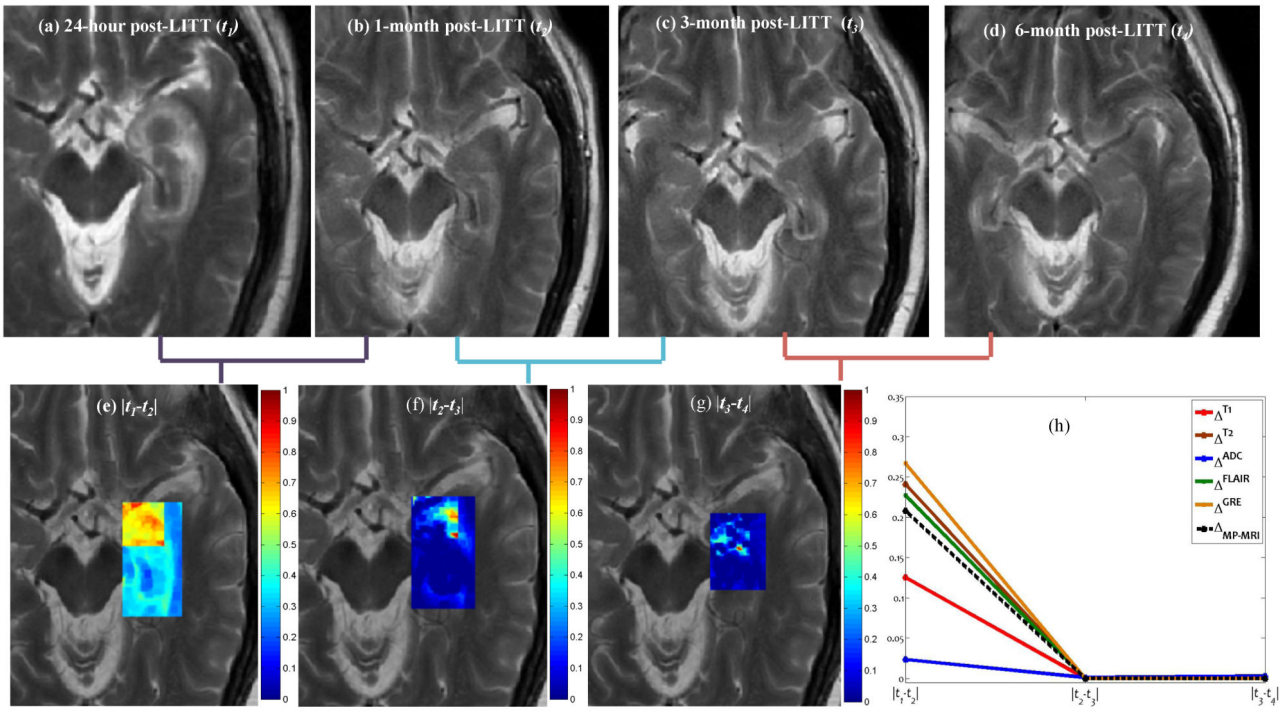

Figure 3.

Original T2-w MRI images for (a) 24-hour, (b) 1-month, (c) 3-month, and (d) 6 month post-LITT. (e)$\tilde{\Delta}_1$(f)$\tilde{\Delta}_{2q}$, and (g)$\tilde{\Delta}_3$, corresponding to difference maps for T2-w MRI computed across subsequent time-points t_1, t_2, t_3, and t_4. Figure 2(h) shows temporal profiles of every MR protocol $i,i \in \{T1,T2,ADC,GRE,FLAIR\}$ reflecting the changes in imaging markers at subsequent time-points.

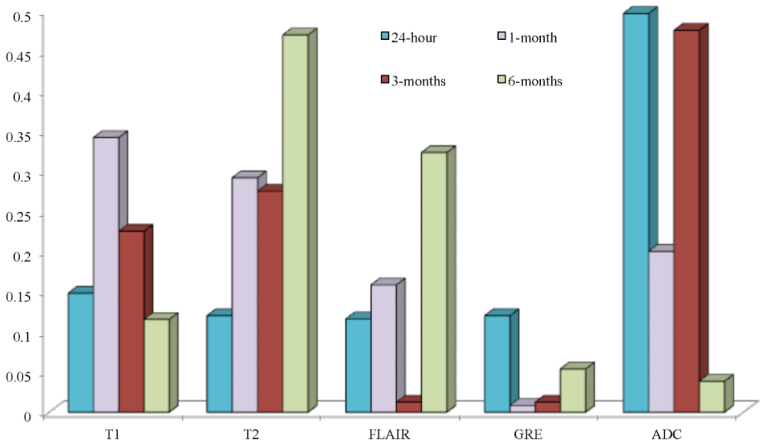

Figure 4.

Contributions of each of the MR protocols (normalized between 0 and 1) in capturing TRC post-LITT at 24-hour, 1-month, 3-month, and 6-month time periods.

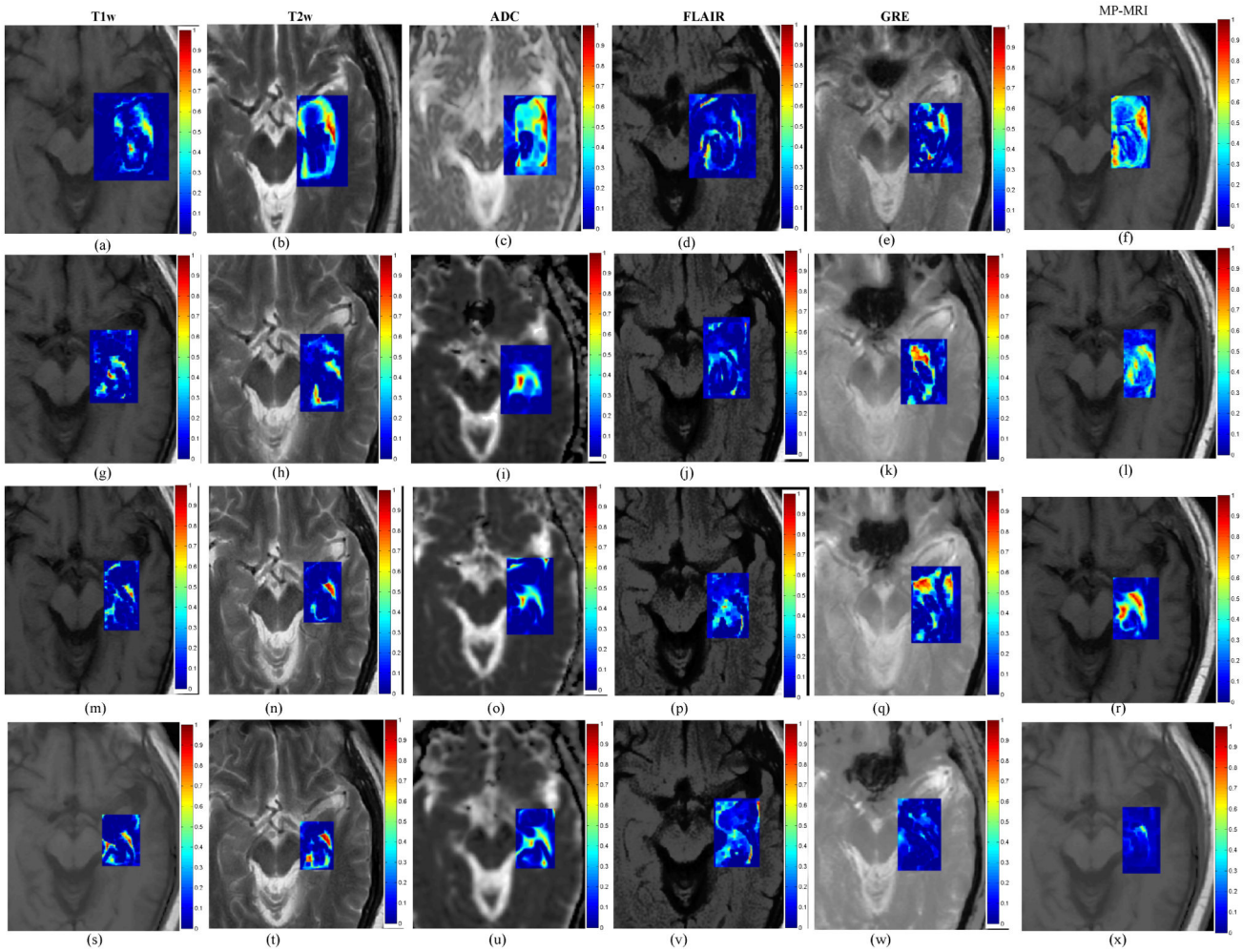

Figure 5.

(a)-(e) difference maps between 24-hours post-LITT and pre-LITT (baseline) for T1-w (a), T2-w (b), ADC (c), FLAIR (d), and GRE (e). Figures 5(g)-(k) show difference maps for 1-month post-LITT with respect to baseline, (m)-(q) show difference maps for 3-month post-LITT with respect to baseline scan, and (s)-(w) show difference maps for 6-month post-LITT with respect to baseline for T1-w, T2-w, ADC, FLAIR and GRE respectively. Corresponding MP-MRI maps obtained by weighted combination of individual MRI protocols are shown in Figures 5(f), (l), (r), (x), corresponding to differences at 24-hour, 1-month, 3-months, and 6-months with respect to baseline scan respectively.

Table 1

Table demonstrating the two datasets and available protocols for follow-up MRIs.

Dataset	MRI Protocols	MRI follow-ups	Status
$\mathbf{D}_1$	T1-w, T2-w, ADC, T2-GRE, T2-FLAIR	24-hours, 1-month, 3-months, 6-months	S.F.
$\mathbf{D}_2$	T1-w, T2-w, ADC, T2-GRE, T2-FLAIR	24-hours, 2-months, 6-months	S.F.

Table 2

List of commonly used notation and symbols in this paper.

Symbol	Description
$C_{T1}^{t_o}$	Baseline (pre-LITT) T1-w MRI scene
i	index for MRI protocol under evaluation, $i \in \{T1, T2, ADC, GRE, FLAIR\}$
$C_i^{t_k}$	Registered i^{th} MRI scene with $C_{T1}^{t_o}$ at time-point k
t_k	Follow-up time-point post-LITT, $k \in \{1, \ldots, n\}$
n	Total number of time-points
G	Ablation zone MRI scene where $G \subset C$
C_i	3D grid of MRI voxels
c	a voxel in C
f_i	intensity at every voxel location c for protocol i
Δ_i^k	Difference map between t_k and t_0 for protocol i, $i \in \{T1, T2, ADC, GRE, FLAIR\}$
$\overset{\sim k}{\Delta i}$	Difference map between t_{k+1} and t_k for protocol i, $i \in \{T1, T2, ADC, GRE, FLAIR\}$
$\mu_i(t_k)$	Average intensity within G computed for Δ_i^k
$\tilde{\mu i}\left(t_k\right)$	Average intensity within G computed for $\overset{\sim k}{\Delta i}$
δ_i	Temporal profile obtained by plotting $\mu_i(t_k)$ at every k for every i
$\tilde{\delta i}$	Temporal profile obtained by plotting $\tilde{\mu i}\left(t_k\right)$ at every k for every i
a_v^k	Individual contribution of each MRI protocol in evaluating TRC at every time-point k
J	Total number of MRI protocols
$\|.\|_1$	L_1-norm
$\|.\|$	Cardinality
N	Cardinality of G
$\mathbf{D}_a$	Patient study, $a \in \{1,2\}$